



Cite this: DOI: 10.1039/d0nj03166f

Stability and decomposition of copper(I) boryl complexes: [(IDipp)Cu–Bneop], [(IDipp*)Cu–Bneop] and copper clusters†‡

 Wiebke Drescher, Corinna Borner and Christian Kleeberg *

The NHC copper boryl complexes [(IDipp)Cu–Bneop] (**2**) and [(IDipp*)Cu–Bneop] (**3**) (IDipp = 1,3-bis(2,6-diisopropylphenyl)imidazol-2-ylidene, IDipp* = 1,3-bis(2,6-(diphenylmethyl)-4-methylphenyl)imidazol-2-ylidene, neop = (OCH₂)₂CMe₂) were synthesised and fully characterised including single crystal X-ray structure determinations. The comparably rapid decomposition of **2**, as reported previously by Sadighi and co-workers, was corroborated and can be attributed to the properties of the Bneop ligand in combination with the steric properties of the IDipp ligand. The decomposition of **2** leads predominantly to the free NHC, the diborane(4) B₂neop₂ (**1**) and, presumably, elemental copper. Minor products of this reductive decomposition are the unprecedented low-valent copper clusters [(IDipp)₆Cu₅] and [(IDipp)₁₂Cu₁₇] that were characterised by single crystal X-ray structure determinations. It is concluded that an insight in the decomposition pathways and products of copper boryl complexes is essential for the understanding of copper boryl complexes and therefor for the further development of the flourishing field of copper mediated borylation reactions.

 Received 23rd June 2020,
 Accepted 27th July 2020

DOI: 10.1039/d0nj03166f

rsc.li/njc

Introduction

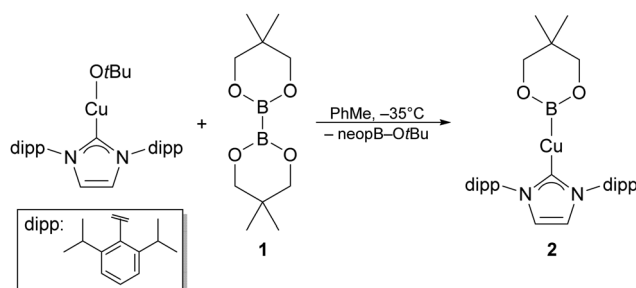
Copper(I) boryl complexes are recognised as central intermediates in copper catalysed borylation reactions with diboranes(4) as boron sources.¹ Since the initial report on those reactions by Miyaura and co-workers in 2001 the formation of a copper boryl complex from a suitable precursor complex and a diborane(4) derivative has been considered central in those reactions.² The first isolated and fully characterized copper boryl complex [(IDipp)Cu–Bpin] (pin = (OCMe₂)₂, IDipp = 1,3-bis(2,6-diisopropylphenyl)imidazol-2-ylidene) was reported in 2005 by Sadighi and co-workers and is since considered as the prototypic copper boryl complex.^{3,4} Nonetheless, in the recent years a number of new copper boryl complexes derived from diboranes(4) have been reported, e.g. with sterically less demanding NHC or phosphine ligands and a variety of dialkoxy and diamino boryl ligands, by our group,^{5,6} as well as with sterically more demanding NHC ligands by Sadighi *et al.* and others.^{7,8}

The three synthetically most broadly employed diborane(4) reagents are undoubtedly B₂pin₂, B₂cat₂ (cat = 1,2-O₂C₆H₄) and

B₂neop₂ (**1**) (neop = (OCH₂)₂CMe₂).¹ The latter one, whilst already introduced in 1994 by Marder and co-workers,⁹ has been somewhat in the shadow of B₂pin₂ and B₂cat₂ but is readily available nowadays.¹

Consistently, the chemistry of copper(I) Bneop complexes is comparably little developed with [(IDipp)Cu–Bneop] (**2**) being the only isolated complex.⁸ This complex was reported by Sadighi *et al.* in 2018 but found to be stable for only less than 20 min at room temperature in solution, as a consequence the complex was only partly characterised (Scheme 1).

This apparent low stability of **2** is unexpected in the light of the generally higher stability of copper boryl complexes with the IDipp ligand (or closely related ligands such as ^{Cl}IDipp = 1,3-bis(2,6-diisopropylphenyl)-4,5-dichloro-imidazol-2-ylidene and



Scheme 1 Formation of [(IDipp)Cu–Bneop] (**2**) from [(IDipp)Cu–OtBu] and B₂neop₂ (**1**) as reported by Sadighi *et al.*⁸

Institut für Anorganische und Analytische Chemie, Technische Universität Braunschweig, Hagenring 30, 38106 Braunschweig, Germany. E-mail: ch.kleeberg@tu-braunschweig.de

† Dedicated to Prof. Dr Todd B. Marder on occasion of his 65th birthday for his outstanding contributions in boron chemistry and in particular transition metal catalysed borylation reactions.

‡ Electronic supplementary information (ESI) available: Additional analytical and structural data. CCDC 2008213–2008218. For ESI and crystallographic data in CIF or other electronic format see DOI: 10.1039/d0nj03166f

SIDipp = 1,3-bis(2,6-diisopropylphenyl)-imidazolidin-2-ylidene) and boryl ligands such as Bpin, Bcat, Bdmab (dmab = 1,2-(NMe)₂C₆H₄) or Bdbab (dbab = 1,2-(NBn)₂C₆H₄).^{3,5,7} In fact the low stability of **2** is more reminiscent to copper boryl complexes with sterically less demanding NHC ligands.⁶

Given our work on reactive, in particular, sterically little demanding NHC copper boryl complexes and their decomposition pathways we endeavoured to (re-)investigate **2** and its sterically more demanding congener [(IDipp*)Cu–Bneop] (**3**) (IDipp* = 1,3-bis(2,6-(diphenylmethyl)-4-methylphenyl)imidazol-2-ylidene).

Results and discussions

Synthesis and characterisation

The reaction of [(IDipp)Cu–OtBu] with B₂neop₂ (**1**) at low temperatures following Sadighi's original procedure furnished [(IDipp)Cu–Bneop] (**2**) (Scheme 1).⁸ An alternative, slightly modified protocol (–35 °C vs. r.t./–40 °C, different handling and work-up) was found to be equally suitable (*vide infra*). However, both procedures led in our hands to varying yields and purities of isolated **2**. Nonetheless, **2** was isolated repeatedly as its PhMe solvate 2(PhMe)_x ($x = 0.22\text{--}0.90$). Whilst the X-ray structure determination (*vide infra*) corroborates the solvate 2(PhMe), elemental analysis and NMR data suggest a gradual removal of the co-crystallised PhMe upon drying *in vacuo* at ambient temperature, possibly accompanied by decomposition.

Despite the low stability of **2** in solution at ambient temperature, as reported by Sadighi and co-workers, we were able to characterise 2(PhMe)_x ($x = 0.75\text{--}0.85$) by ¹H and ¹³C NMR spectroscopy at –40 °C as well as at room temperature, although the latter was accompanied by severe decomposition (*vide infra*).

We concluded that increasing the steric demand of the NHC ligand should increase the stability of the NHC copper Bneop complex. We chose the established complex [(IDipp*)Cu–OtBu] as the starting material, essentially replacing the iso-propyl groups of the IDipp ligand by diphenylmethyl groups (Scheme 2).^{10e}

Indeed, the complex [(IDipp*)Cu–Bneop] (**3**) can be isolated upon reaction of [(IDipp*)Cu–OtBu] with **1** reproducibly in 70% isolated yield and is much more stable than its leaner congener **2** (Fig. S3, ESI†).¹³ In line with that, so far no boryl complexes of Bneop could be isolated using other NHC ligands such as

1,3-bis(*tert*-butyl)imidazol-2-ylidene or 1,3-bis(iso-propyl)imidazol-4,5-dimethyl-2-ylidene, that we have successfully employed to obtain related copper(I) boryl complexes.^{6b}

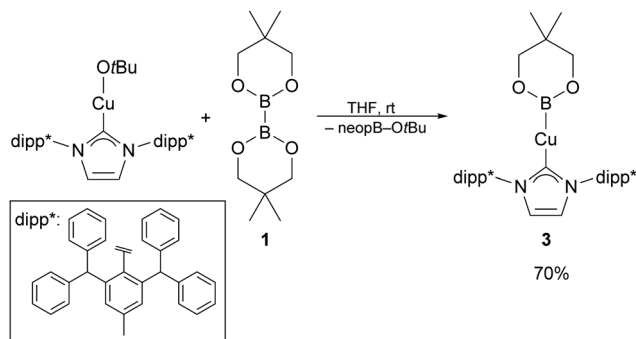
For **2** at room temperature a very broad singlet signal at 40 ppm ($\Delta w_{1/2} = 3510$ Hz) was observed in the ¹¹B{¹H} NMR spectrum, whereas at –40 °C no signal was observed due to the excessive line broadening.¹¹ For **3** however no ¹¹B NMR signal was unambiguously identified even at room temperature. Which is rationalised with the reduced transverse relaxation time (T_2), and therefore even larger linewidths than observed for **2** for less flexible and mobile **3**.

For **2**, however, the NMR data are in line with the ¹¹B NMR chemical shifts observed for related mononuclear NHC copper boryl complexes such as [(IDipp)Cu–Bpin] 41.7 ppm,³ [(SIDipp)Cu–Bcat] 45 ppm ($\Delta w_{1/2} = 1700$ Hz),^{5b} and [(IDipp)Cu–Bdmab] 44.1 ppm ($\Delta w_{1/2} = 1020$ Hz).^{5a} The same is true for the carbene carbon ¹³C NMR shifts of 186.5 ppm and 187.0 ppm of **2** and **3**, respectively, that compare well with those of [(IDipp)Cu–Bpin] 187.2 ppm,³ and [(IDipp)Cu–Bdmab] 187.1 ppm.^{5a}

Solid-state structures

Single crystals of **2** were obtained from PhMe/*n*-pentane and from THF/*n*-pentane at –40 °C as the solvates 2(PhMe) and 2(THF), respectively. 2(PhMe) forms colourless plates and comprises two independent molecules in the asymmetric unit in a triclinic unit cell in $P\bar{1}$ ($Z = 4, Z' = 2$). Whereas 2(THF) forms colourless needles and comprises only one molecule in the asymmetric unit in the monoclinic unit cell in $P2_1/n$ ($Z = 4, Z' = 1$) (Fig. S6, ESI†).¹³ In 2(PhMe) the two independent molecules A and B of **2** form chains along the *b* axis, with H···O and H···π interactions as the most pronounced intermolecular interactions (Fig. 1). A Hirshfeld surface analysis reveals that besides the ubiquitous H···H contacts with minimal d_i and d_e of 0.9–1.1 Å (surface area: A 88.8%, B 80.1%) the 2D fingerprint plots exhibit two distinct features (Fig. 1).¹² Most pronounced are the H···O contacts (surface area: A 5.6%, B 4.2%) with very distinct sharp features in the 2D fingerprint plots with minimal $d_i + d_e$ of 2.1–2.2 Å. Whilst generally analogous, the H···O interactions realised in the two independent molecules are slightly different as evidenced by the unsymmetrical 2D fingerprint plots as well as slightly different d_i and d_e distances (*vide infra*).¹³ Less pronounced, but in agreement with the data reported for polycyclic aromatic hydrocarbons are the H···C contacts (surface area: A 11.6%, B 12.6%) with the minimal $d_i + d_e$ around 2.6 Å associated with the H···π interaction H2···Ct1A and H3A'···Ct1 (Fig. S4, ESI†).^{12a,13}

The H···O interactions are also illustrated by the short H···O distance of H3···O2A 2.24 Å and H2A···O1' 2.35 Å as well as the angles C3···H3···O2A 172.9° and C2A···H2A···O1' 161.1° (Fig. 1). Although, these data must be considered with some care due to the use of a riding model in the refinement of the hydrogen atoms, it can certainly be stated that the distances are short compared to the sum of the respective van-der-Waals radii of 2.64 Å.¹⁴ The intramolecular C_{Carbene}–Cu and B–Cu distances and the B–Cu–C_{Carben} angles (Fig. 1) are in line with the respective data for [(IDipp)Cu–Bpin] (C–Cu 1.937(2) Å, B–Cu 2.002(3) Å, C–Cu–B 168.1(2)°) and [(SIDipp)Cu–Bcat] (C–Cu 1.930(1) Å, B–Cu 1.984(2) Å,



Scheme 2 Formation of [(IDipp*)Cu–Bneop] (**3**) from [(IDipp*)Cu–OtBu] and B₂neop₂ (**1**).

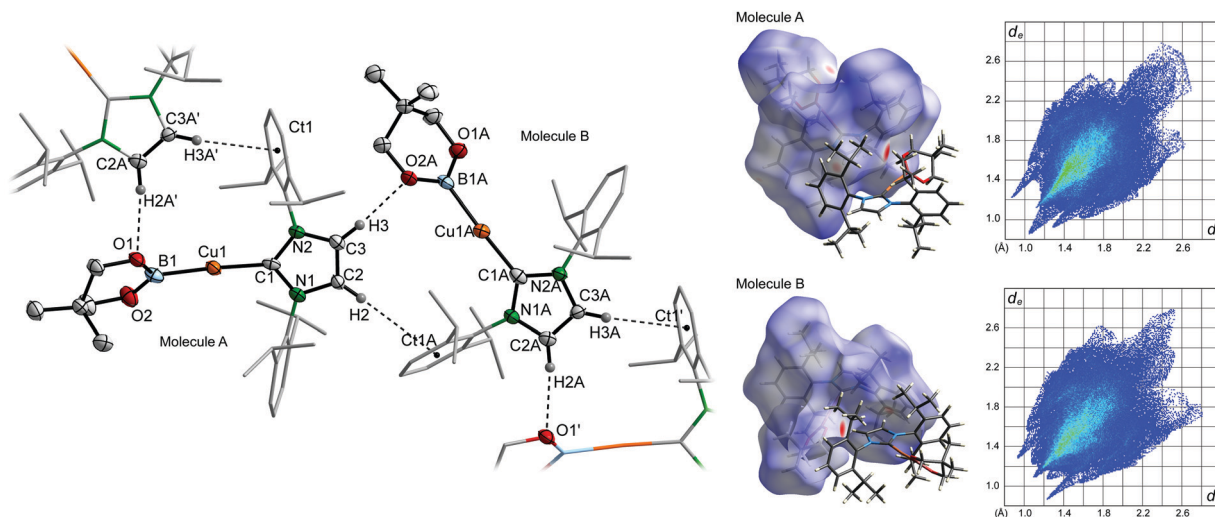


Fig. 1 Section of the solid state structure of [(IDipp)Cu-Bneop] (**2**) from **2**(PhMe) (left) and Hirshfeld surface analysis data (right); ellipsoids at the 50% probability level, selected H and C atoms shown with arbitrary radius. Selected distances (Å) and angles (°): C1–Cu1 1.932(4), B1–Cu1 2.007(6), H3···O2A 2.240(4), C3···O2A 3.185(6), H2···Ct1A 3.1819(4), B1–Cu1–C1 174.8(2), C3···H3···O2A 172.9(2), $\angle_{(N,C,N,Cu)/(O,B,O,Cu)}$ 47.4(3); C1A–Cu1A 1.928(5), B1A–Cu1A 2.000(5), H2A···O1' 2.351(4), C2A···O2A 3.265(6), H3A···Ct1' 2.816(3), B1–Cu1–C1 174.6(2), C2A···H2A···O1' 161.1(3), $\angle_{(N,C,N,Cu)/(O,B,O,Cu)}$ 45.5(8).

C–Cu–B 172.52(7)°).^{3,5b} The interplanar angles $\angle_{(N,C,N,Cu)/(O,B,O,Cu)}$, however, exhibit much more variation amongst these three complexes ([[(IDipp)Cu-Bpin] 40.0°, [[(SIDipp)Cu-Bcat] 71.9(2)°] (Fig. 1).^{3,5b}

The THF solvate **2**(THF) exhibits comparable geometrical properties as the PhMe solvate. In particular, an analogous chain packing motif with distinct H···O and H··· π interactions is observed; albeit the inter chain interactions are different (Fig. S6 and S7, ESI†).¹³

Single crystals of **3** were obtained from an ethereal solution by slow evaporation at room temperature under an inert atmosphere. **3** forms colourless laths with one molecule in the asymmetric unit in an orthorhombic unit cell in *Pbca* ($Z = 8$, $Z' = 1$).^{13,15} The Hirshfeld surface analysis reveals that H···H contacts with minimal d_i and d_e of 0.9 Å (surface area: 72.8%) and H···C contacts (surface area: 24.4%) are the most pronounced interactions (Fig. 2 and Fig. S5, ESI†).¹³ Whereas, as an effect of the increased steric shielding of the ligand and in contrast to the structures of **2**(PhMe) and **2**(THF), intermolecular H···O contacts are only marginal (surface area: 1.3%, $d_i + d_e > 2.5$ Å).¹³ The molecular geometry with respect to the C_{Carbene} –Cu and B–Cu distances and the B–Cu– C_{Carbene} angles are, however, in line with the respective data for **2** and other IDipp/SIDipp boryl complexes (*vide supra*). The interplanar angle $\angle_{(N,C,N,Cu)/(O,B,O,Cu)}$ is with 82.6°, in contrast to the IDipp/SIDipp boryl complexes (*vide supra*), almost rectangular, certainly an effect of the increased steric encumbrance of **3**.

Stability and decomposition

The decomposition of **2** is readily followed by *in situ* ¹H and ¹¹B{¹H} NMR spectroscopy (Fig. 3 and Fig. S1a, ESI†).¹³ As reported for other NHC copper boryl complexes the decomposition is quite selective.^{6b} The ¹H NMR spectra show the formation of essentially two species, one with a neop scaffold

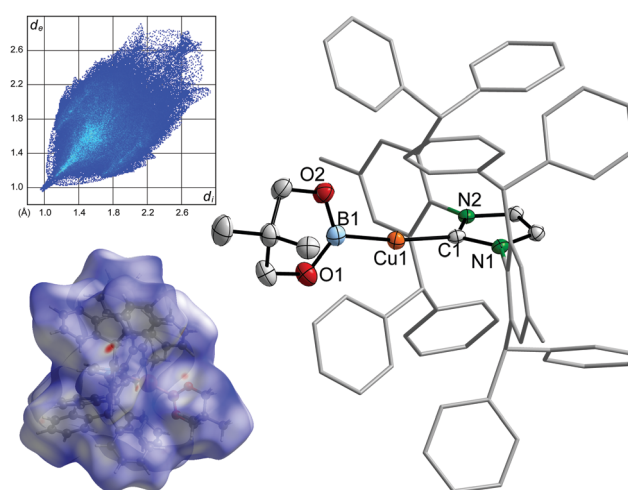


Fig. 2 Molecular structure of [(IDipp)Cu-Bneop] (**3**) and Hirshfeld surface analysis data (insets); ellipsoids at the 50% probability level, H atoms are omitted for clarity. Selected distances (Å) and angles (°): C1–Cu1 1.935(2), B1–Cu1 2.020(2), B1–Cu1–C1 171.36(8), $\angle_{(N,C,N,Cu)/(N,B,N,Cu)}$ 82.6(6).

and one with an IDipp scaffold. The corresponding ¹¹B NMR data exhibit however, two signals. Comparison with an authentic sample of the diborane(**4**) indicates that **1** is the neop based decomposition product detected by ¹H NMR spectroscopy and is also identified in the ¹¹B{¹H} NMR spectrum (28.8 ppm, $\Delta\omega_{\frac{1}{2}} = 240$ Hz). Moreover, **1** has occasionally been deposited as single crystals from solution of decomposed **2**, as verified by unit cell determination.

However, the second signal at 17.7 ppm ($\Delta\omega_{\frac{1}{2}} = 130$ Hz) indicates the presence of a second boron containing species, possibly a four coordinate boric acid derivative, *e.g.* the spiro borate [Bneop₂][–] (*vide infra*). The second species in the ¹H NMR spectrum is not as readily assigned, the NMR signals of an

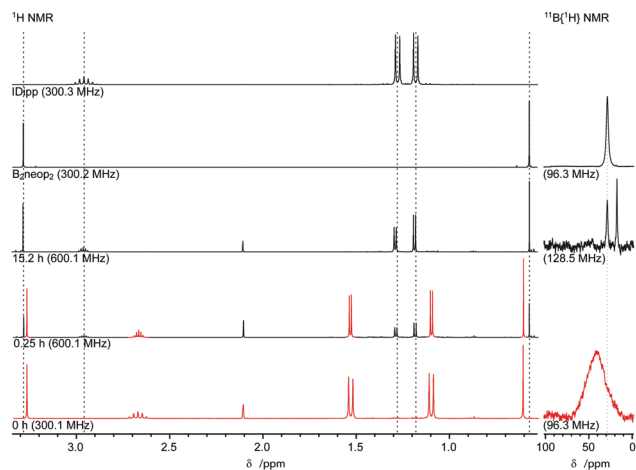


Fig. 3 Decomposition of **2** monitored by NMR spectroscopy (C_6D_6 , r.t.).¹¹

authentic sample of the free carbene IDipp does not quite fit to the signals of the decomposition product. However, considering the very small deviations and the observation of the free NHC ligand as decomposition product of other boryl complexes it may be concluded that the small deviations are caused by concentration effects and/or weak dynamic coordination to one of the boron containing decomposition products. The kinetics of the decomposition appears to be in agreement with the report of substantial decomposition after 20 min by Sadighi *et al.*⁸ The *in situ* 1H NMR data of the decomposition suggests a half-life of **2** in C_6D_6 solution at room temperature of about 1.5 h (Fig. S1b, ESI \ddagger).¹³ The decomposition of **2** is further accompanied by the formation of a dark precipitate. Though this could not be isolated, it may be concluded to be elemental copper, in line with the findings with other NHC copper boryl complexes.^{6b} A powder diffraction pattern recorded of the dark residue obtained after drying of a solution of *in situ* generated and decomposed **2** *in vacuo* supports the formation of the free carbene IDipp and **1** as the major decomposition products. However, no clear evidence for the formation of elemental copper or low-valent copper clusters (*vide infra*) was obtained (Fig. S2, ESI \ddagger).¹³

Finally it may be concluded, that the decomposition of **2** is surprisingly fast in comparison to the stability of the congeners $[(IDipp)Cu-Bpin]$, $[(^{Cl}IDipp)Cu-Bpin]$, $[(SIDipp)Cu-Bcat]$, $[(IDipp)Cu-Bdmab]$ and $[(IDipp)Cu-Bdbab]$.^{3,5,7} The decomposition pathway, however, appears generally to be comparable to the one observed for sterically little encumbered NHC copper boryl complexes, leading to the symmetrical diborane(4) derivative **1** as oxidative coupling product and, presumably, the free NHC and elemental copper.

However, in several instances additional decomposition products were obtained in minuscule amounts but in single crystalline form (*vide infra*).

In contrast to **2**, the steric more encumbered complex **3** does not exhibit any significant decomposition within 16 h at room temperature (Fig. S3, ESI \ddagger).¹³ Hence, the stability of copper boryl complexes depends on both the steric properties of the auxiliary, NHC, ligand as well as the properties of the boryl ligand. This agrees

nicely with our earlier findings that sterically little encumbered NHC copper boryl complexes are extremely unstable.^{6b} Furthermore, the observed packing pattern in the solid-state structures of **2** including distinct intermolecular $H \cdots O$ interactions suggests a certain accessibility of the Bneop moiety and is in line with a higher reactivity/lower stability of this complex.

Additional decomposition products of **2**

During the studies on **2** three different additional decomposition products $[(IDipp)_2Cu][Bneop_2]$, $[(IDipp)_6Cu_{55}]$ and $[(IDipp)_{12}Cu_{179}]$ were repeatedly, although not very reproducibly obtained as a few single crystals. The cationic *bis*-NHC copper(I) complex $[(IDipp)_2Cu][Bneop_2]$, was obtained performing the reaction of $[(IDipp)Cu-OtBu]$ with **1** in THF. The formation of spiroborates as a side-product of reactions of diboranes(4) has been observed earlier, though, in particular with B_2cat_2 .^{5b,16}

As this complex is a copper(I) complex and as such likely not associated with the reductive decomposition of **2**, it is not discussed here any further.¹³

The remarkable metalloid cluster $[(IDipp)_6Cu_{55}]$ was repeatedly obtained from reaction mixtures of **1** and $[(IDipp)Cu-OtBu]$ in PhMe or C_6D_6 at room temperature, whereas $[(IDipp)_{12}Cu_{179}]$ was repeatedly obtained from THF/*n*-pentane or Et_2O/n -pentane solution at room temperature. It has to be emphasised that both clusters were obtained only in minuscule amounts and only in about 30% of the – apparently identical – experiments, and are solely characterised by single crystal X-ray determinations. Nonetheless, both complexes have been obtained repeatedly and even from two different solvents. Whilst ongoing work is directed towards a preparative access to these clusters, the structures of these clusters may be discussed here due to their relevance for the decomposition of **2**.

The copper atoms in the cluster $[(IDipp)_6Cu_{55}]$ adopt – approximately – icosahedral symmetry (Fig. 4). It may be dissected in an inner shell comprising of a centred – slightly distorted – icosahedron of copper atoms (Cu_{13}) and an outer shell comprising of 42 copper atoms.¹³ The outer shell itself comprises an icosahedron of copper atoms (Cu_{12}) with additional copper atoms in the middle of all icosahedron edges (Cu_{30}) (Fig. 4, right). Crystallographically the cluster does not exhibit icosahedral symmetry but is situated only on a centre of inversion in a spacegroup of the type $P\bar{1}$ ($Z = 1$, $Z' = \frac{1}{2}$).

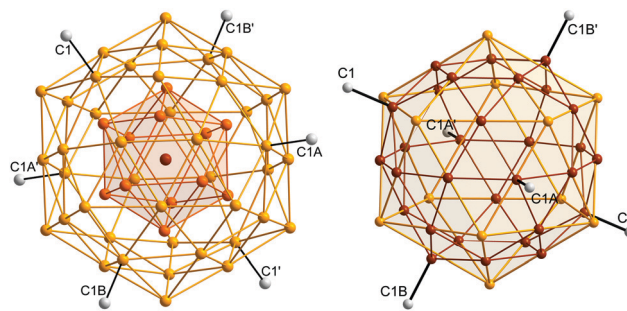


Fig. 4 Left: Views of Ball and Stick model of $[(IDipp)_6Cu_{55}]$. Right: Ball and Stick of the outer shell of $[(IDipp)_6Cu_{55}]$. NHC only represented by their carbene carbon atoms (grey).¹³

The carbene carbon atoms of the six, pairwise equivalent, IDipp ligands form an approximate octahedron, coordinating non-icosahedron copper atoms. The coordinated copper atoms are slightly displaced from their idealised positions on the middle of icosahedron edges. The Cu··Cu distances are between 2.39 Å, found between the inner and outer icosahedra along the approximate fivefold axis, and 2.72 Å involving copper atoms coordinated by an IDipp ligand. Nonetheless, the average Cu··Cu distance around 2.55 Å (Fig. S9, ESI†) agrees well with that in elemental copper of 2.56 Å.¹⁷ The C_{NHC}-Cu distances are with a range of 1.94–1.98 Å slightly longer than those in IDipp and SIDipp copper boryl complexes (*vide supra*), where typically distances of around 1.93 Å are found.^{3,5} The structure of [(IDipp)₆Cu₅₅] is related to that one of the mixed NHC/phosphine copper cluster [(Me₂IPr)₁₀Cu₂₃(PMe₃)₂] in so far, as both clusters comprise centred copper icosahedra as central motif. The latter one, however, comprises 10 additional copper atoms above the 10 trigonal equatorial faces.^{6b} Moreover, both the Cu··Cu and the C_{NHC}-Cu distances in the latter cluster are comparable with those in [(IDipp)₆Cu₅₅].^{6b} It should be further mentioned that centred icosahedra are also realised in the low-valent copper hydrido clusters [Cu₂₅H₂₂(PPh₃)₁₂]Cl and [Cu₂₉Cl₄H₂₂(Ph₂phen)₁₂]Cl,¹⁸ and, moreover, similar icosahedral structures are discussed for the pivotal gold cluster [Au₅₅(PPh₃)₁₂Cl]₆.¹⁹ It is also worth noting that copper monolayers with bound NHC ligands have been reported recently.²⁰

[(IDipp)₁₂Cu₁₇₉] crystallises in the monoclinic spacegroup type *P*₂₁/*n* and is situated on an inversion centre, however, the cluster itself does not appear to possess inversion symmetry, resulting in extensive disorder of the copper atoms within [(IDipp)₁₂Cu₁₇₉]. Similar as [(IDipp)₆Cu₅₅] the bigger cluster may be dissected into different shells. The inner core consists of 2 equivalent copper atoms (C54 and C54') one of them centring an icosahedron, the other comprising an apical position of this icosahedron. This latter copper atom, however, centres again a two-fold base-capped pentagonal prism (Fig. 5, inset). Due to the

centre of inversion present, the middle pentagon Cu1w–Cu5w is disordered over two positions and so is this entire Cu₁₉ motif. Consequently, the entire Cu₁₇₉ cluster is not centrosymmetric and possess only one approximate five-fold axis (*vide infra*). This disorder then propagates through the 2nd (52 Cu atoms) and 3rd/outer (107 Cu atoms) shell of this cluster (Fig. 5 and Fig. S10, S11, ESI†).¹³ This account so far for 178 copper atoms, one additional copper atom is found disordered over 10 pairwise symmetry equivalent positions on the surface of the Cu₁₇₈ motif.²¹ Finally, the 12 NHC ligands coordinate 12 copper atoms of the outer shell, obeying inversion symmetry. The structure of this copper cluster as discussed here is one interpretation of this disorder and is disputable; for a detailed reasoning leading to this structure see the ESI† provided.¹³ It is also noted that the Cu₅₅ cluster motif as found in [(IDipp)₆Cu₅₅] is also found as a partial motif in [(IDipp)₁₂Cu₁₇₉] (around Cu54, Fig. S12, ESI†).¹³

The Cu··Cu distances in the cluster [(IDipp)₁₂Cu₁₇₉] cover a range from 2.35 to 2.70 Å with a maxima around 2.55 Å and thus are comparable with those found in [(IDipp)₆Cu₅₅] (Fig. S13, ESI†).¹³ The C_{NHC}-Cu distances that are in a range of 1.93–1.97 Å and, hence, also comparable to those in [(IDipp)₆Cu₅₅].

In summary, it is stated that the decomposition of 2 leads to remarkable and unprecedented metalloid copper clusters. That complements our results on the sterically little encumbered NHC and phosphine copper boryl complexes, where also – smaller – copper clusters have been observed as decomposition products.⁶ Finally, it must be emphasised, that those copper clusters are subject of ongoing studies and that they have so far been only characterised by X-ray crystallography. Hence, it cannot be fully excluded that additional hydrido ligands are present, undetected due to their low scattering power. Moreover, for both clusters co-crystallised solvent was found that could not be adequately refined and was removed mathematically.¹³ However, none of the solvent molecules was close to the cluster Cu atoms, excluding an additional solvent coordination. The single crystal X-ray structure determinations were for both clusters, but in particular for [(IDipp)₁₂Cu₁₇₉], not straightforward and must be considered with the necessary care.¹³

Conclusion

IDipp copper boryl complexes have gained considerable attention as prototypic copper boryl model complexes since their introduction by Sadighi and co-workers.³ However, the first complexes of the Bneop ligand, [(IDipp)Cu–Bneop] (2), has only recently been reported – though not comprehensively characterised – and exhibits a comparable low stability in solution.⁸ The Bneop complexes [(IDipp)Cu–Bneop] (2) and the sterically more encumbered [(IDipp*)Cu–Bneop] (3) are isolated and thoroughly characterised by multinuclear NMR spectroscopy in solution as well as structurally in the solid state by single crystal X-ray diffraction. Both the spectroscopic data as well as the structural data do not exhibit significant differences to those of other IDipp copper boryl complexes. The, indeed, rapid decomposition of 2 was found to lead to predominantly the free NHC ligand and B₂neop₂ (1) and,

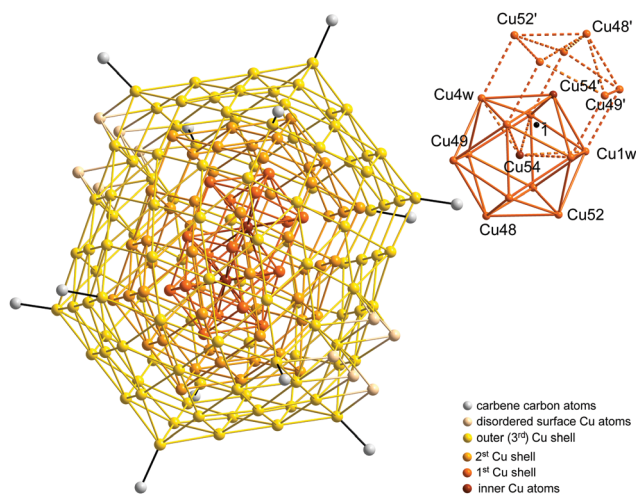


Fig. 5 Left: Views of Ball and Stick model of [(IDipp)₁₂Cu₁₇₉]; NHC only represented by the carbene carbon atoms.¹³ Inset: detail of the inner core of [(IDipp)₁₂Cu₁₇₉].

presumably, elemental copper. Whereas **3** does not show appreciable decomposition under comparable conditions. The destabilisation of **2** compared to other IDipp copper boryl complexes appears to be an intrinsic effect of the Bneop ligand but can be compensated by the use of the sterically more demanding IDipp* ligand. Besides the mentioned decomposition products of **2** the two remarkable copper clusters [(IDipp)₆Cu₅₅] and [(IDipp)₁₂Cu₁₇₉] were obtained occasionally in miniscule amounts as single crystals. This shows, together with our earlier reports,⁶ that the formation of low-valent copper clusters is a relevant decomposition pathway of copper boryl complexes. This and the possible role and mechanistic implications of those clusters have to be considered in the further development of the flourishing field of copper mediated borylation reactions.

Experimental part

General considerations

[(IDipp)Cu–OtBu]^{10a,b} and [(IDipp*)Cu–OtBu]^{10c-e} were prepared according to literature procedures, however, KOtBu was substituted for NaOtBu throughout the synthesis. All other compounds were commercially available and were used as received; their purity and identity was checked by appropriate methods. All solvents were dried using MBraun solvent purification systems, deoxygenated using the freeze–pump–thaw method and stored under purified nitrogen. All manipulations were performed using standard Schlenk techniques under an atmosphere of purified nitrogen or in a nitrogen-filled glove box (MBraun). NMR spectra were recorded on Bruker Avance II 300, Avance III HD 300, Avance III 400, Avance III 500 or Avance 600 spectrometers. For air sensitive samples NMR tubes equipped with screw caps (WILMAD) were used and the solvents were dried over potassium/benzophenone and degassed. Chemical shifts (δ) are given in ppm, using the (residual) resonance signal of the solvents for calibration (C₆D₆: ¹H NMR: 7.16 ppm, ¹³C NMR: 128.06 ppm, THF-d₈: ¹H NMR: 1.72 ppm, ¹³C NMR: 25.31 ppm).²² ¹¹B chemical shifts are reported relative to BF₃·Et₂O. ¹³C and ¹¹B NMR spectra were recorded employing composite pulse ¹H decoupling. 2D NMR techniques were employed if necessary to assign the individual signals (¹H–¹H NOESY (1 s mixing time), ¹H–¹H COSY, ¹H–¹³C HSQC and ¹H–¹³C HMBC). Unless noted otherwise, Melting points were determined in flame-sealed capillaries under nitrogen using a Büchi 535 apparatus and are not corrected. Elemental analyses were performed at the Institut für Anorganische und Analytische Chemie of the Technische Universität Braunschweig using an Elementar vario MICRO cube instrument.

X-ray diffraction studies

The single crystals were transferred into inert perfluoroether oil inside a nitrogen-filled glovebox and, outside the glovebox, rapidly mounted on top of a human hair, Mitegen loop or a Hampton loop and placed in the cold nitrogen gas stream on the diffractometer.^{23a} The data were either collected on a Rigaku Oxford Diffraction Synergy-S or an Oxford Diffraction

Nova A instrument, using mirror-focused CuK α radiation. The reflections were indexed, integrated and appropriate absorption corrections were applied as implemented in the CrysAlisPro software package.^{23b} The structures were solved employing the program SHELXT and refined anisotropically for all non-hydrogen atoms by full-matrix least squares on all F^2 using SHELXL software.^{23c-e} Unless noted otherwise hydrogen atoms were refined employing a riding model; methyl groups were treated as rigid bodies and were allowed to rotate about the E–CH₃ bond. During refinement and analysis of the crystallographic data the programs WinGX, OLEX,² PLATON/SQUEEZE, Mercury and Diamond were used.^{23f-j} Unless noted otherwise the shown ellipsoids represent the 50% probability level and hydrogen atoms are omitted for clarity. Adapted numbering schemes may be used to improve the readability.

Synthetic procedures

[(IDipp)Cu–Bneop] (**2**). Complex **2** was prepared following Sadighis procedure.⁸ Alternatively the procedure given below was employed. Though both procedures yielded repeatedly pure **2**, both procedures are in our hands not very reliable with respect to the obtained yields and the purity of the compounds. Moreover, we were unable to perform the reaction successfully at a larger scale. [(IDipp)Cu–OtBu] (50.0 mg, 95 μ mol, 1.0 eq.) was dissolved in PhMe (2 mL) in a screw-cap vial and a suspension of **1** (21.5 mg, 95 μ mol, 1.0 eq.) in PhMe (0.5 mL) was added at ambient temperature in the dark. After 5 min of shaking PhMe was added until a clear solution is obtained (ca. 2.5 mL). The by now dark solution was left to crystallise at –40 °C for 36 h to obtain the solvate **2**(PhMe) in crystalline form suitable for X-ray diffraction analysis. The supernatant mother liquor was decanted and the residues washed with *n*-pentane (3 \times 2 mL) and dried briefly *in vacuo* to obtain **2**(PhMe)_{>0.8}, in agreement with the ¹H NMR data (10.5 mg, 16 μ mol, 17% as **2**(PhMe)). **2**(PhMe) obtained may be recrystallised from THF/*n*-pentane at –40 °C to obtain single-crystals of **2**(THF) suitable for X-ray diffraction analysis.

M.p. Decomposition to black material above 75 °C. Found: C, 70.51; H, 8.27; N, 4.31. Found: C, 68.11; H, 7.95; N, 4.71 (prolonged drying). Found: C, 67.66; H, 8.36; N, 4.82 (very long drying). Calc. for C₁₂H₁₆B₂O₄ (**2**): C, 68.02; H, 8.21; N, 4.96. Calc. for C₃₂H₄₆BCuN₂O₂ (**2**(PhMe)): C, 71.27; H, 8.28; N, 4.26. Calc. for C_{36.6}H_{51.3}BCuN₂O₂ (**2**(PhMe)_{3/2}): C, 70.29; H, 8.26; N, 4.47. Calc. for C_{35.5}H₅₀BCuN₄O₄ (**2**(PhMe)_{3/2}): C, 69.77; H, 8.25; N, 4.58. δ_{H} (500.3 MHz, THF-d₈, –40 °C) 0.64 (6 H, s, C(CH₃)₂), 1.20 (12 H, d, J = 6.9 Hz, CH(CH₃)₂), 1.33 (12 H, d, J = 6.8 Hz, CH(CH₃)₂), 2.61 (4 H, sept., J = 6.8 Hz, CH(CH₃)₂), 3.02 (4 H, s, CH₂), 7.30 (4 H, d, J = 7.7 Hz, 3-CH_{Ar}), 7.42 (2 H, s, NCH), 7.43 (2 H, t, J = 7.7 Hz, 4-CH_{Ar}). δ_{C} (125.8 MHz, THF-d₈, –40 °C) 23.1 (C(CH₃)₂), 23.8 (CH(CH₃)₂), 25.6 (CH(CH₃)₂), 29.5 (CH(CH₃)₂), 31.9 (C(CH₃)₂), 70.1 (CH₂), 123.6 (NCH), 124.3 (3-CH_{Ar}), 130.4 (4-CH_{Ar}), 136.2 (1-C_{Ar}), 146.5 (2-C_{Ar}), 186.5 (C_{Carbene}). δ_{B} (160.5 MHz, THF-d₈, –40 °C) No ¹¹B NMR signal was detected. Sample composition according to ¹H NMR integration **2**(PhMe)_{0.85}. δ_{H} (600.1 MHz, C₆D₆, r.t.) 0.61 (6 H, s, C(CH₃)₂),

1.10 (12 H, d, $J = 6.9$ Hz, $\text{CH}(\text{CH}_3)_2$), 1.54 (12 H, d, $J = 6.8$ Hz, $\text{CH}(\text{CH}_3)_2$), 2.67 (4 H, sept., $J = 6.9$ Hz, $\text{CH}(\text{CH}_3)_2$), 3.27 (4 H, s, CH_2), 6.22 (2 H, s, NCH), 7.07 (4 H, d, $J = 7.8$ Hz, 3- CH_{Ar}), 7.14 (2 H, t, $J = 7.9$ Hz, 4- CH_{Ar}). δ_{C} (150.9 MHz, C_6D_6 , r.t.) 23.0 ($\text{C}(\text{CH}_3)_2$), 23.7 ($\text{CH}(\text{CH}_3)_2$), 25.4 ($\text{CH}(\text{CH}_3)_2$), 29.1 ($\text{CH}(\text{CH}_3)_2$), 31.6 ($\text{C}(\text{CH}_3)_2$), 70.0 (CH_2), 121.9 (NCH), 124.0 (3- CH_{Ar}), 129.03 (4- CH_{Ar}), 135.3 (1- C_{Ar}), 145.9 (2- C_{Ar}), C_{Carbene} was not detected. δ_{B} (96.3 MHz, C_6D_6 , r.t.) 40 (br. s, $\Delta w_{\frac{1}{2}} = 3500$ Hz).¹¹ Sample composition according to ^1H NMR integration 2(PhMe)_{0.75}.

[(**IDipp***)Cu-Bneop] (3). [(**IDipp***)Cu-OtBu] (26.7 mg, 25.4 μmol , 1.0 eq.) and 1 (5.7 mg, 25.4 μmol , 1.0 eq.) were combined and dissolved in THF (2 mL). After approximately five minutes at room temperature, all volatiles were removed under reduced pressure. The oily residue was washed with *n*-pentane (3 \times 2 mL) at room temperature and dried *in vacuo* to give 3 (19.5 mg, 17.9 μmol , 70%) as a pale yellow solid. Single crystals were obtained by evaporation of an ethereal solution of 3 at room temperature under inert conditions.

M.p. Decomposition to black material above 189 °C. Found: C, 80.78; H, 6.30; N, 2.82. Calc. for $\text{C}_{74}\text{H}_{66}\text{BCuN}_2\text{O}_2$ (3): C, 81.56; H, 6.10; N, 2.57. Repeated attempts to obtain a more satisfactory elemental analysis failed. δ_{H} (300.1 MHz, C_6D_6 , r.t.) 0.78 (6 H, s, $\text{C}(\text{CH}_3)_2$), 1.60 (6 H, s, 4- $\text{C}_{\text{Ar}}-\text{CH}_3$), 3.48 (4 H, s, CH_2), 5.53 (2 H, s, NCH), 5.77 (4 H, s, $\text{CH}(\text{C}_{\text{Ph}})_2(\text{C}_{\text{Ar}})$), 6.99 (4 H, s, 3- CH_{Ar} , overlapping), 6.99 (20 H, s, CH_{Ph} , overlapping), 7.13 (4 H, app. t, $J = 7.6$ Hz, 4- CH_{Ph}), 7.36 (8 H, app. t, $J = 7.7$ Hz, 3- CH_{Ph}), 7.73 (8 H, d, $J = 7.7$ Hz, 2- CH_{Ph}). δ_{C} (100.7 MHz, C_6D_6 , r.t.) 21.2 (4- $\text{C}_{\text{Ar}}-\text{CH}_3$), 23.2 ($\text{C}(\text{CH}_3)_2$), 31.7 ($\text{C}(\text{CH}_3)_2$), 51.7 (s, $\text{CH}(\text{C}_{\text{Ph}})_2(\text{C}_{\text{Ar}})$), 70.3 (CH_2), 122.8 (NCH), 126.6 (s, 4- CH_{Ph}), 126.8 (s, 4- CH_{Ph}), 128.5 (s, 3- CH_{Ph}), 129.0 (s, 3- CH_{Ph}), 130.0 (s, 2- CH_{Ph}), 130.6 (s, 3- CH_{Ar}), 130.8 (s, 2- CH_{Ph}), 135.2 (s, 1- C_{Ar}), 140.1 (s, 4- C_{Ar}), 141.7 (s, 1- C_{Ph}), 143.5 (s, 2- C_{Ar}), 144.1 (s, 1- C_{Ph}), 187.0 (C_{Carbene} , $^1\text{H}-^{13}\text{C}$ HMBC only). δ_{B} (160.5 MHz, C_6D_6 , r.t.) No ^{11}B NMR signal was detected.

[(**IDipp**)₆Cu₅₅]. The synthesis of 2 was conducted as described above, but instead of crystallisation at -40 °C the dark reaction mixture was left at room temperature under inert condition for several days. In about 30% of the attempts miniscule amounts of small (longest axis < 0.1 mm) dark black prisms had deposited that were analysed by single crystal X-ray structure determination.

[(**IDipp**)₁₂Cu₁₇₉]. A saturated solution of 2 in Et_2O (0.5 mL) was layered with *n*-pentane (2 mL) at room temperature. After a few days at room temperature a dark precipitate had formed. In about 30% of the attempts, additionally miniscule amounts of small (longest axis < 0.1 mm) dark prisms had deposited that were analysed by single crystal X-ray structure determination.

Conflicts of interest

There are no conflicts to declare.

Acknowledgements

C. K., C. B. and W. D. gratefully acknowledges support by a Research Grant (KL 2243/5-1) of the Deutsche Forschungsgemeinschaft (DFG). The authors thank AllyChem Co. Ltd. for a generous gift of B_2neop_2 .

Notes and references

- For reviews see: (a) L. Dang, Z. Lin and T. B. Marder, *Chem. Commun.*, 2009, 3987; (b) J. Cid, H. Gulyás, J. J. Carbó and E. Fernández, *Chem. Soc. Rev.*, 2012, **41**, 3558; (c) E. C. Neeve, S. J. Geier, I. A. I. Mkhaliid, S. A. Westcott and T. B. Marder, *Chem. Rev.*, 2016, **116**, 9091; (d) J. Cid, J. J. Carbó and E. Fernández, *Chem. – Eur. J.*, 2012, **18**, 12794.
- K. Takahashi, T. Ishiyama and N. Miyaura, *J. Organomet. Chem.*, 2001, **625**, 47.
- D. S. Laitar, P. Müller and J. P. Sadighi, *J. Am. Chem. Soc.*, 2005, **127**, 17196.
- Besides copper boryl complexes derived from diborane(4) derivatives, and hence of direct relevance for copper catalysed borylation reactions, copper boryl complexes have also been obtained from boryl lithium species: (a) T. Kajiwara, T. Terabayashi, M. Yamashita and K. Nozaki, *Angew. Chem., Int. Ed.*, 2008, **47**, 6606; (b) Y. Okuno, M. Yamashita and K. Nozaki, *Eur. J. Org. Chem.*, 2011, 3951; (c) Y. Segawa, M. Yamashita and K. Nozaki, *Angew. Chem., Int. Ed.*, 2007, **46**, 6710.
- (a) C. Borner and C. Kleeberg, *Eur. J. Inorg. Chem.*, 2014, 2486; (b) W. Drescher and C. Kleeberg, *Inorg. Chem.*, 2019, **58**, 8215.
- (a) C. Borner, L. Anders, K. Brandhorst and C. Kleeberg, *Organometallics*, 2017, **36**, 4687; (b) C. Kleeberg and C. Borner, *Organometallics*, 2018, **37**, 4136.
- (a) K. Semba, M. Shinomiya, T. Fujihara, J. Terao and Y. Tsuji, *Chem. – Eur. J.*, 2013, **19**, 7125; (b) C. M. Wyss, J. Bitting, J. Bacsá, T. G. Gray and J. P. Sadighi, *Organometallics*, 2016, **35**, 71.
- A. J. Jordan, P. K. Thompson and J. P. Sadighi, *Org. Lett.*, 2018, **20**, 5242.
- (a) P. Nguyen, G. Lesley, N. J. Taylor, T. B. Marder, N. L. Pickett, W. Clegg, M. R. J. Elsegood and N. C. Norman, *Inorg. Chem.*, 1994, **33**, 4623; (b) F. J. Lawlor, N. C. Norman, N. L. Pickett, E. G. Robins, P. Nguyen, G. Lesley, T. B. Marder, J. A. Ashmore and J. C. Green, *Inorg. Chem.*, 1998, **37**, 5282; (c) W. Clegg, M. R. J. Elsegood, F. J. Lawlor, N. C. Norman, N. L. Pickett, E. G. Robins, A. J. Scott, P. Nguyen, N. J. Taylor and T. B. Marder, *Inorg. Chem.*, 1998, **37**, 5289; (d) M. Eck, S. Würtemberger-Pietsch, A. Eichhorn, J. H. J. Berthel, R. Bertermann, U. S. D. Paul, H. Schneider, A. Friedrich, C. Kleeberg, U. Radius and T. B. Marder, *Dalton Trans.*, 2017, **46**, 3661.
- (a) L. Hintermann, *Beilstein J. Org. Chem.*, 2007, **3**, 22; (b) V. Jarkauskas, J. P. Sadighi and S. L. Buchwald, *Org. Lett.*, 2003, **5**, 2417; (c) M. Hans, J. Lorkowski, A. Demonceau and L. Delaude, *Beilstein J. Org. Chem.*, 2015, **11**, 2318; (d) W.-J. Yoo, T. V. Q. Nguyen and S. Kobayashi, *Angew. Chem., Int. Ed.*, 2014, **53**, 10213; (e) J. Zhai, A. S. Filatov, G. L. Hillhouse and M. D. Hopkins, *Chem. Sci.*, 2016, **7**, 589.
- To unambiguously identify the very broad ^{11}B NMR signal of 2 the spectrum was processed by subtraction of a suitable background spectrum. A Lorentz type window function (LB = 30 Hz) was used. C. Kleeberg, A. G. Crawford, A. S. Batsanov, P. Hodgkinson, D. C. Apperley, M. S. Cheung, Z. Lin and T. B. Marder, *J. Org. Chem.*, 2012, **77**, 785.

- 12 (a) M. A. Spackman and J. J. McKinnon, *CrystEngComm*, 2002, **4**, 378; (b) M. A. Spackman and D. Jayatilaka, *CrystEngComm*, 2009, **11**, 19.
- 13 See ESI† for details.
- 14 M. Mantina, A. C. Chamberlin, R. Valero, C. J. Cramer and D. G. Truhlar, *J. Phys. Chem. A*, 2009, **113**, 5806.
- 15 It is noted that the solvate $3(\text{C}_6\text{D}_6)_2$ crystallises from benzene solutions. However, due to extensive twinning and the low over-all quality of the crystals a satisfactory structure refinement was not obtained. The cell parameters are: a 11.0712(6) Å, b 26.527(2) Å, c 26.606(2) Å, α 67.203(7)°, β 85.754(6)°, γ 89.877(3)°, $P\bar{1}$, $Z = 4$, $Z' = 2$.
- 16 W. Clegg, M. R. J. Elsegood, A. J. Scott, T. B. Marder, C. Dai, N. C. Norman, N. L. Pickett and E. G. Robins, *Acta Crystallogr.*, 1999, **C55**, 733.
- 17 R. W. G. Wyckoff, *Cryst. Struct.*, 1963, **1**, 7.
- 18 (a) T.-A. D. Nguyen, Z. R. Jones, B. R. Goldsmith, W. R. Buratto, G. Wu, Z. L. Scott and T. W. Hayton, *J. Am. Chem. Soc.*, 2015, **137**, 13319; (b) T.-A. D. Nguyen, Z. R. Jones, D. F. Leto, G. Wu, S. L. Scott and T. W. Hayton, *Chem. Mater.*, 2016, **28**, 8385.
- 19 (a) Y. Pei, N. Shao, Y. Gao and X. C. Zeng, *ACS Nano*, 2010, **4**, 2009; (b) N. Jian, C. Stapelfeldt, K.-J. Hu, M. Fröba and R. E. Palmer, *Nanoscale*, 2015, **7**, 885.
- 20 C. R. Larrea, C. J. Baddeley, M. R. Narouz, N. J. Mosey, J. H. Horton and C. M. Crudden, *ChemPhysChem*, 2017, **18**, 3536.
- 21 It was considered that this electron density might represent hydrido ligand(s). The observed distances of the electron density maxima to the cluster Cu atoms in a range of 2.25–2.55 Å are more suggestive for Cu atoms than for hydrogen atoms, as crystallographically determined Cu–H distances for $\mu_{\geq 2}$ -hydrogen atoms are typically below 2 Å. CSD database Version 5.41, May 2020C. R. Groom, I. J. Bruno, M. P. Lightfoot and S. C. Ward, *Acta Crystallogr.*, 2016, **B72**, 171.
- 22 G. R. Fulmer, A. J. M. Miller, N. H. Sherden, H. E. Gottlieb, A. Nudelman, B. M. Stoltz, J. E. Bercaw and K. I. Goldberg, *Organometallics*, 2010, **29**, 2176.
- 23 (a) D. Stalke, *Chem. Soc. Rev.*, 1998, **27**, 171; (b) CrysAlisPro, Rigaku Oxford Diffraction, Versions 1.171.37.35, 1.171.40.21a, 2014–2018; (c) G. M. Sheldrick, *Acta Crystallogr.*, 2015, **A71**, 3; (d) G. M. Sheldrick, *Acta Crystallogr.*, 2008, **A64**, 112; (e) G. M. Sheldrick, *Acta Crystallogr.*, 2015, **C71**, 3; (f) L. J. Farrugia, *J. Appl. Crystallogr.*, 2012, **45**, 849; (g) O. V. Dolomanov, L. J. Bourhis, R. J. Gildea, J. A. K. Howard and H. Puschmann, *J. Appl. Crystallogr.*, 2009, **42**, 339; (h) A. L. Spek, *Acta Crystallogr.*, 2015, **C71**, 9; (i) C. F. Macrae, I. Sovago, S. J. Cottrell, P. T. A. Galek, P. McCabe, E. Pidcock, M. Platings, G. P. Shields, J. S. Stevens, M. Towler and P. A. Wood, *J. Appl. Crystallogr.*, 2020, **53**, 226; (j) Diamond – Crystal and Molecular Structure Visualization, Crystal Impact - H. Putz and K. Brandenburg GbR, Bonn, Germany, 2020.